

Statistical Characterisation & Classification of Edge Localised Plasma Instabilities

A. J. WEBSTER¹, R. O. DENDY^{1,2}, AND JET EFDA CONTRIBUTORS*

JET-EFDA, Culham Science Centre, Abingdon, OX14 3DB, UK.

¹*EURATOM/CCFE Fusion Association, Culham Science Centre,
Abingdon, Oxfordshire, OX14 3DB, UK. and*

²*Centre for Fusion, Space and Astrophysics, Department of Physics,
Warwick University, Coventry CV4 7AL, UK.*

(Dated: February 27, 2013)

PACS numbers: 52.35.Py, 05.45.Tp, 52.55Dy

* See the Appendix of F. Romanelli et al., Proceedings of the 24th IAEA Fusion Energy Conference 2012, San Diego, US.

Abstract

The statistics of edge-localised plasma instabilities (ELMs) in toroidal magnetically confined fusion plasmas are considered. From first principles, standard experimentally motivated assumptions are shown to determine a specific probability distribution for the waiting times between ELMs: the Weibull distribution. This is confirmed empirically by a statistically rigorous comparison with a large data set from the Joint European Torus (JET). The successful characterisation of ELM waiting times enables future work to progress in various ways. Here we present a quantitative classification of ELM types, complementary to phenomenological approaches. It also informs us about the nature of ELMing processes, such as whether they are random or deterministic.

Introduction: Edge localised plasma instabilities (ELMs) [1–4] are almost ubiquitous in high performance magnetically confined fusion (MCF) plasmas. Their phenomenological properties are correlated with the quality of global energy confinement, and the peak energy fluxes onto material surfaces [3–6]. Key challenges are to statistically characterise these processes sufficiently well that a quantitative distinction between different observed classes of ELMs becomes possible, and to relate this classification to the physical processes responsible for them. This will provide a test for theoretical models, and is an important step towards improved estimates for the distribution of ELM waiting times and sizes, both of which must be controlled in reactor-scale MCF plasma experiments.

ELMs offer a rich and diverse experimental phenomenology [1–8]. There is intense theoretical research on the instabilities that may be responsible for triggering them [9], but few unifying principles have been identified. We will show that widely held experimentally motivated assumptions about ELMing require particular statistical characteristics. Specifically, if one assumes that the likelihood of ELM occurrence increases monotonically with time elapsed since the most recent ELM, then the measured distribution of waiting times between ELMs should belong to a broad class of probability density functions (pdfs) of which the Weibull distribution [10] is a special case. This physical approach contrasts with a trial and error search for a function that best fits the data [11].

To test this conjecture requires the identification and selection of a large representative data set, the development and use of a reliable ELM detection algorithm, and a method to find and compare the best possible fits between data and any proposed pdf. This will provide a rigorous basis for present and future studies. As an application of our analysis, we distinguish between type I and type III ELMs in a set of plasmas from the Joint European Torus (JET) tokamak[12], on the basis of ELM waiting time statistics alone. Whereas type III ELMs are usually smaller than type I ELMs, typically they are more frequent and the plasma’s energy confinement is lower. The ELM type is presently determined by the ELM frequency’s response to heating[2–4]. The physically motivated derivation for our pdf allows a clear physical interpretation of our statistical classification.

Theoretical Background: Consider the sequence and distribution of time intervals (waiting times) between ELMs. After an ELM, at $t = 0$, we discuss the statistical properties of the time of the next ELM in terms of two linked functions. We define $p(t)dt$ to be the probability that the next ELM is in the time interval $(t, t + dt)$, given that it has not yet

occurred at time t . This differs crucially from the pdf of time intervals between ELMs, which we denote by $P(t)$, and gives the fraction of inter-ELM time intervals that are between t and $(t + dt)$ as $P(t)dt$. Clearly $p(t)dt$ is a conditional probability which, multiplied by the probability that no ELM occurs between $t = 0$ and t , yields the probability $P(t)dt$ of an inter-ELM time interval between t and $t + dt$. This gives the identity:

$$P(t) = p(t) \left\{ 1 - \int_0^t P(y)dy \right\} \quad (1)$$

which allows $p(t)$ to be expressed in terms of $P(t)$. Alternately, Eq. 1 can be used to show that,

$$P(t) = -\frac{d}{dt} \exp \left\{ - \int_0^t p(y)dy \right\} \quad (2)$$

giving $P(t)$ as a function of $p(t)$, with $\int_0^\infty P(t)dt = 1$. The equivalence of Eqs. 1 and 2 can be confirmed by substituting Eq. 2 into Eq. 1, or by writing Eq. 1 as, $p(t) = -(d/dt) \ln \left(1 - \int_0^t P(y)dy \right)$, and substituting into Eq. 2.

We adopt the experimentally motivated ansatz that for a short time period t_m immediately after an ELM, $p(t) = 0$, beyond which it starts to increase. The simplest dimensionless representation of this hypothesis is,

$$p(t)dt = \begin{cases} 0 & t < t_m \\ \beta \left(\frac{t-t_m}{t_0} \right)^{\beta-1} \frac{dt}{t_0} & t \geq t_m \end{cases} \quad (3)$$

where t_0 sets the time scale. Using Eq. 2, this gives,

$$P(t)dt = \begin{cases} 0 & t < t_m \\ \beta \left(\frac{t-t_m}{t_0} \right)^{\beta-1} \exp \left[- \left(\frac{t-t_m}{t_0} \right)^\beta \right] \frac{dt}{t_0} & t \geq t_m \end{cases} \quad (4)$$

This is a Weibull distribution [10]. It is specified by two dimensionless parameters β and $\alpha = t_m/t_0$, the time scale being set by t_0 . From a theoretical perspective, the values $\beta = 1$ and $\beta = 2$ deserve special mention. Beyond a possible time delay t_m , for $\beta = 1$, $p(t)$ is constant, corresponding to a “memoryless” process in which events occur with equal probability independent of time. The transition between $p(t)$ being a concave (decreasing derivative) and convex (increasing derivative) function is at $\beta = 2$. As β increases, events appear increasingly regular. The preceding derivation assumes that events are independent and that the process causing them is stationary.

Data sets: Eq. 4 will provide a good fit to a measured sequence of waiting times when the hypothesis represented by Eq. 3 holds. Such distributions have a single maximum, and require a macroscopic plasma equilibrium with a quasi-stationary ELMing process. Pdfs with additional maxima that are unlikely to have arisen from noise were discarded, as were data whose ELM type was uncertain. A search of carbon-wall JET data yielded a selection of 70 type I and 15 type III ELM data sets. The data sets each have a steady period of ELMy H-mode lasting between 3 and 6 seconds, and plasmas with an energy confinement time typically between 0.25 and 0.4 seconds. The data sets are listed in the supplementary material (SM) [13]. The need for quasi-stationary ELM statistics is met by the pulse length and quality of the JET plasmas studied, which is much improved on the 4 data sets studied in [11].

ELM detection: ELM detection algorithms typically examine the radiation associated with ELMs, using a threshold in amplitude to signal the start of an ELM, and a similar threshold or combination of thresholds to determine when an ELM has finished [11]. In those respects, our detection algorithm is the same. The advance of the algorithm described here is that the thresholds are determined from the data in a precise and statistically invariant way, so that we do not need to reset thresholds for different sets of data. This allows statistically robust comparisons between different data sets, and enables the technique to be used for non-steady-state and real-time situations if desired. Our algorithm examines the signal intensity of the Lyman-alpha radiation from Deuterium (D_α) at JET's inner divertor, and proceeds in two steps. First a scan is made of the data, obtaining for each time point the box-average and standard deviation of the signal intensity for a time interval T immediately prior to that point. The average and standard deviation determine a Gaussian distribution, that is subsequently used to distinguish ELMs automatically. For this study the (D_α) signal threshold for ELM-detection was for signal intensities that would only occur one time in twenty, based on the Gaussian distribution obtained from the data preceding the measurement in question. Once the signal has fallen below the average again, the ELM is considered to have finished. We use a time interval $T = 0.41\text{s}$ that is much longer than the time between ELMs, but is reasonably short compared with changes to the plasma equilibrium. For stationary pulses such as those here, with ELM waiting times $t \ll T$, results are unchanged by increasing T to the time duration of the entire dataset. For cases such as these, T is independent of the data. Because we are interested in classifying ELMs

by their statistical properties, here we chose the same threshold for both the type I and III data. The threshold of one in twenty was sufficiently sensitive for type III data, but kept noise tolerable in type I data. A systematic exploration of these thresholds will be presented elsewhere.

The method just described provides a non-subjective method to determine when the D_α signal intensity indicates an ELM. Because the study involves the detection and study of many thousands of ELMs, “incorrect” detection or omission of one or more ELMs becomes part of the experimental noise. The detection settings require only one value to be set in advance of an analysis, and because it does not need to be changed or optimised for any given set of data, it is easy and quick to analyse very large data sets. Also because thresholds are set independently of the data, it is possible to systematically mine noisy data by varying the noise and time-scale parameters to search for patterns in data that would otherwise be obscured.

Best fit & goodness of fit: Both the Weibull and Gaussian distributions have free parameters that must be chosen to fit the data. A simple fit is provided by using the moments of the data, *e.g.* average, standard deviation, and skewness, to fit the parameters. More rigorously, we can consider the likelihood function for the probability of the data given the model being considered [14] (*e.g.* the Weibull model, W), and parameters $\bar{\lambda}$, with,

$$L(\bar{\lambda}) = P(\{t_i\}|W, \bar{\lambda}) \quad (5)$$

where $P(\{t_i\}|W, \bar{\lambda})$ is the probability of observing the set of waiting times $\{t_i\}$, given the assumption of a Weibull distribution (W), with fitting parameters $\bar{\lambda}$. The free parameters that maximise $L(\bar{\lambda})$ are their maximum likelihood (ML) estimate [14], for which the likelihood of the data (given the distribution being considered), is a maximum. In practice the ML estimates are found by starting from the moment-fitted estimates and iterating to find $\bar{\lambda}$ that maximises $L(\bar{\lambda})$. Given the best fits for two distributions P_A and P_B , we can compare their goodness of fit by calculating their likelihood ratio [14],

$$\Lambda(P_A, P_B) = \frac{P(\{t_i\}|P_A, \bar{\lambda}_A)}{P(\{t_i\}|P_B, \bar{\lambda}_B)} \quad (6)$$

Under the assumption of independent $\{t_i\}$, the likelihood function and likelihood ratio can be expanded, with for example, $P(\{t_i\}|P_A, \bar{\lambda}_A) = \prod_{i=1}^n P(t_i|P_A, \bar{\lambda}_A)$. Whether P_A or P_B is a better fit to the data is determined by whether Λ is greater, or less, than 1.

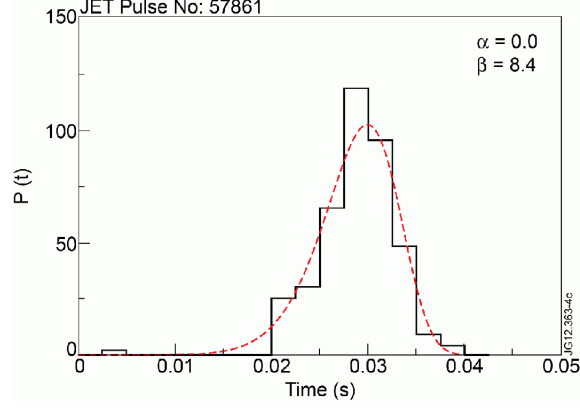


FIG. 1: Weibull (blue) and experimental pdfs (black bar chart), for JET pulse no. 57861 (type I ELMs).

Eq. 4 has one more free parameter than a Gaussian. Thus although Eq. 4 might provide a best fit to the data, the model might not be better, because the fit used an extra parameter. A Bayesian analysis would introduce an extra factor [14] in Eq. 6 to account for this. However its influence will reduce, as the number of ELM time intervals increases. Unless the factor is of order $1/\Lambda$ it will not affect the decision for which is the best fit. For the classification of data, the most important issue is that the pdf (not the model), is a good fit. From that perspective the issue is not relevant. Eq. 6 rigorously indicates which pdf is the best fit, and for the large number of ELMs in our analyses, Eq. 6 is sufficient to determine whether the model is significantly better or worse than a Gaussian.

An absolute measure of goodness of fit, is provided by dividing the ELM waiting time axis into intervals, calculating the fraction P_i of observed ELMs in each interval i , and calculating the co-efficient of variation $c_W = \langle (P_i - P_W(t_i))^2 \rangle / \langle P_W(t_i) \rangle^2$ between the observed (P_i) and the theoretical ($P_W(t_i)$) values at the midpoint t_i of the interval. This gives a normalised measure of the difference between the observed and theoretical pdfs, and provides an absolute measure for goodness of fit. It has the disadvantage of being dependent upon the number of data points used to generate the P_i . Small numbers of points will make c_W susceptible to noise, increasing its value. The choice of time intervals will also affect c_W , and consequently affect a fit that minimises c_W . With enough data this would no longer be the case, but in practice it prevents c_W from determining a unique best fit. For these reasons we use a maximum likelihood best fit, which is unique. Similarly if c_W is used to determine which

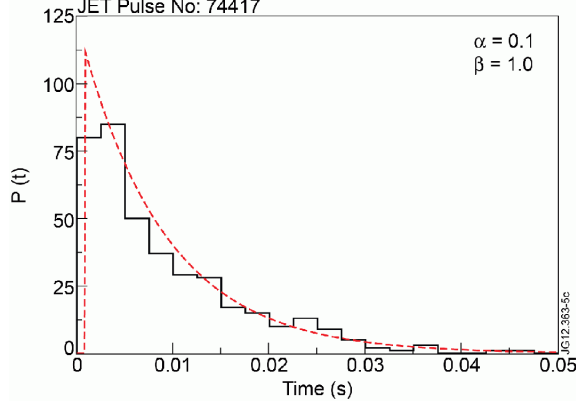


FIG. 2: Weibull (blue) and experimental pdfs (black bar chart), for JET shot no. 74417 (type III ELMs).

pdf gives the best fit, the decision is in practice influenced by the choice of time intervals.

ELM Classification: A full listing of the datasets studied, the time intervals over which they were analysed, and the results from their analysis are presented in the SM [13]. For a dataset with n ELMs, we substitute Eq. 4 for P_A and a Gaussian for P_B in Eq. 6, then calculate the geometric mean $\Lambda^{1/n}$ which will be of order 1. If $\Lambda^{1/n}$ is greater (less) than 1.0 then Λ will be much larger (smaller) for $n \gg 1$, indicating whether the Weibull is a better (worse) fit than a Gaussian. For the type I datasets $\langle \Lambda^{1/n} \rangle = 1.01 \pm 0.04$, where the error of ± 0.04 is the standard deviation, and $n \sim 100$. Using time intervals of 2.5×10^{-3} s, the coefficient of variation between the fitted and observed pdfs is $\langle c_W \rangle = 0.63 \pm 0.22$ for the Weibull best fits, and $\langle c_G \rangle = 0.63 \pm 0.20$ for the Gaussian best fits. For the type III datasets $\langle \Lambda^{1/n} \rangle = 1.51 \pm 0.15$, with $n \sim 300$ or larger, $\langle c_W \rangle = 0.70 \pm 0.23$, and $\langle c_G \rangle = 1.25 \pm 0.24$. Typical examples are in Figs. 4 and 5. Whereas the fits are similarly good for type I ELMs, the Weibull distribution is the clear best fit for type III ELMs. Substantially improved fits are likely if outliers are removed by improved data, improved ELM detection techniques, or with some algorithm. The values of c_W and c_G can be reduced if the best fit minimises them instead of Λ .

Figure 6 plots α and β for the type I and type III ELM datasets. There is a clear clustering of type III data for $\beta = 1$ and $\alpha < 0.5$. As noted earlier, $\beta = 1$ has special significance because beyond an initial time delay t_m , it corresponds to a “memoryless” process in which the probability of an ELM is independent of time. The type I data has a wide spread in

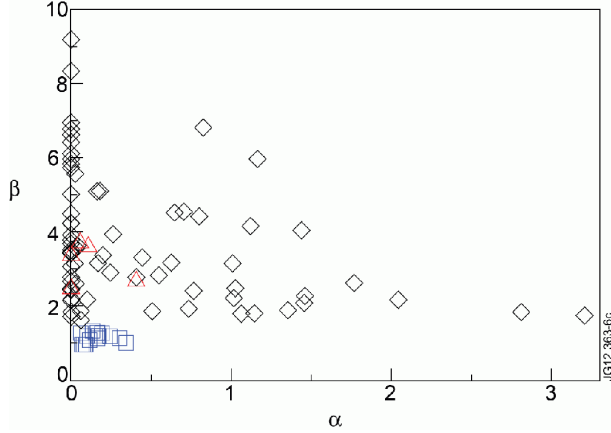


FIG. 3: Maximum-likelihood best fits to Eq. 4: type I ELM database (black diamonds), type III database (blue squares), and some high frequency ELMs (red triangles). Type III data is characterised by $\beta \sim 1$, whereas all other data has $\beta \gtrsim 2$.

α and β , but notably β remains of order 2 or larger. As β increases, ELMs will appear increasingly regular. Therefore the type I ELMs studied here are consistent with a process whereby the probability of an ELM increases with time since the previous ELM, possibly due to the build-up of some physical quantity with time. The similarly good agreement between the Gaussian and Weibull fits allows the alternative interpretation that type I ELMs have a specific frequency that is broadened by noise, and that the good fit to type III ELM data is coincidental. This is possible, although our original hypothesis is consistent with present ELM models, and explains the good fit to both the type I and type III data. To avoid disagreement about the classification of ELM types, our dataset excludes ELMs whose type is uncertain. Therefore it is possible that there is a continuum between the classifications that would not be observed in our data set of typical type I and type III ELMs.

As an example we analysed JET plasmas 66105-66109, whose ELM frequency is typical of type III ELMs[2–4, 6], but whose D_α signal is visually similar to that of type I ELMs. Based on Fig. 6, they are not type III ELMs.

Conclusions: We have shown how simple experimentally motivated assumptions require a Weibull pdf for inter-ELM waiting times. The model applies to stationary processes. A search of JET data yielded 64 sufficiently long and steady plasmas to test the model, details of which are in the SM [13]. A statistically rigorous ELM detection technique was developed to compare the data sets from experiments many years apart. The method uses a single

dimensionless threshold that is set independently of the data, and a single time-period, allowing rapid objective comparisons between different data sets. The dataset was analysed, and a maximum likelihood best fit calculated, finding a good Weibull fit to both type I and type III data. Therefore we explored whether the dimensionless fitting co-efficients α and β could be used to classify the data, concluding that they can. The classification has a clear interpretation - type III ELMs are consistent with a memoryless process, but type I ELMs are consistent with the build-up of a quantity with time, leading to instability. In contrast, present ELM classification requires either a subjective judgment, or experimental time to determine how ELM frequency responds to heating [2–4].

To summarise, we have shown that a rigorous statistical analysis of ELM waiting times is possible, that it can provide a quantitative classification of ELM types, and physical insight into the processes responsible for them. The methods have numerous potential future applications, especially for the longer plasma pulses planned for ITER[15]. These include data mining, use in real-time and for other signals, and a quantitative characterisation of the response of ELM sequences to external parameters.

Acknowledgments: Thanks to B. Alper, G. Maddison, & M. Beurskens for advice on ELM data. This work, supported by the European Communities under the contract of Association between EURATOM and CCFE, was carried out within the framework of the European Fusion Development Agreement. The views and opinions expressed herein do not necessarily reflect those of the European Commission. This work was also part-funded by the RCUK Energy Programme under grant EP/I501045. We acknowledge the UK EPSRC for support.

-
- [1] M. Keilhacker, Plasma Phys. Control. Fusion 26, 49 (1984)
 - [2] H. Zohm, Plasma Phys. Control. Fusion 38, 105 (1996)
 - [3] A. Loarte *et al.*, Plasma Phys. Control. Fusion 45, 1549 (2003)
 - [4] K. Kamiya *et al.*, Plasma Phys. Control. Fusion 49, S43 (2007)
 - [5] D.C. McDonald *et al.*, Fusion Sci. Technol. 53, 891, (2008)
 - [6] J. Rapp *et al.*, Nucl. Fusion 49, 095012, (2009)
 - [7] Y. Liang, Fusion Sci. Technol. 59, 586, (2011)

- [8] A.W. Degeling *et al.*, Plasma Phys. Control. Fusion 43, 1671, (2001)
- [9] A.J. Webster, Nucl. Fusion 52, 114023, (2012)
- [10] W. Weibull, Transactions of the American Society of Mechanical Engineers, September issue, 293-297, (1951)
- [11] J. Greenhough, S.C. Chapman, R.O. Dendy, and D.J. Ward, Plasma Phys. Control. Fusion 45, 747 (2003)
- [12] J. Wesson, *Tokamaks* (Oxford University Press, Oxford, 1997)
- [13] See supplementary material at [] for full details of the datasets studied and the results of their analysis.
- [14] D.S. Sivia, *Data Analysis A Bayesian Tutorial* (Oxford University Press, Oxford, 2005)
- [15] R. Aymar *et al.* for THE ITER TEAM, Plasma Phys. Control. Fusion 44, 519 (2002)

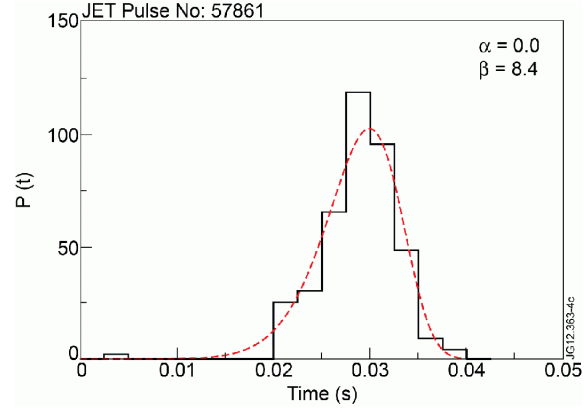


FIG. 4: Weibull (blue) and experimental pdfs (black bar chart), for JET pulse no. 57861 (type I ELMs).

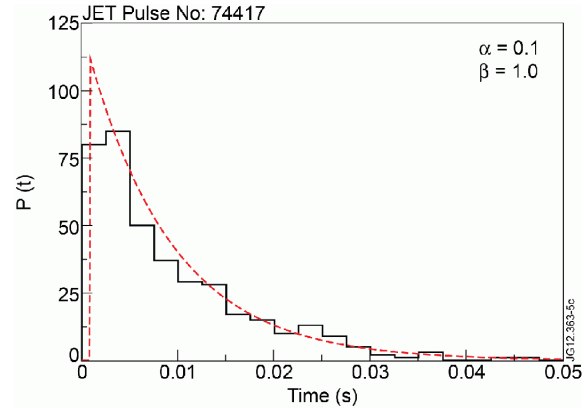


FIG. 5: Weibull (blue) and experimental pdfs (black bar chart), for JET shot no. 74417 (type III ELMs).

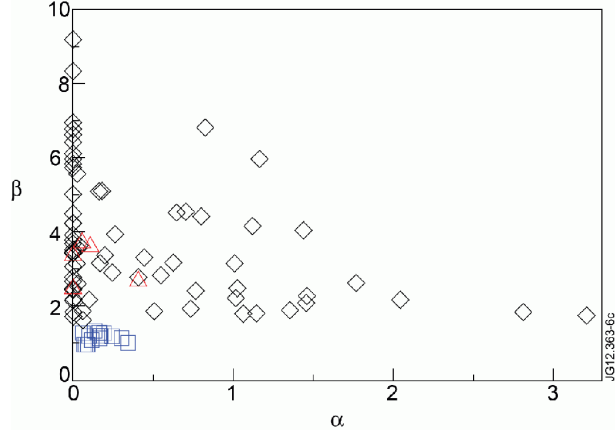


FIG. 6: Maximum-likelihood best fits to Eq. 4: type I ELM database (black diamonds), type III database (blue squares), and some high frequency ELMs (red triangles). Type III data is characterised by $\beta \sim 1$, whereas all other data has $\beta \gtrsim 2$.

Supplementary Material for Statistical Characterisation and Classification of Edge Localised Plasma Instabilities

A. J. WEBSTER¹, R. O. DENDY^{1,2}, AND JET EFDA CONTRIBUTORS*

¹*EURATOM/CCFE Fusion Association, Culham Science Centre,
Abingdon, Oxfordshire, OX14 3DB, UK. and*

²*Centre for Fusion, Space and Astrophysics, Department of Physics,
Warwick University, Coventry CV4 7AL, UK.*

PACS numbers: 52.35.Py, 05.45.Tp, 52.55Dy

* See the Appendix of F. Romanelli et al., Proceedings of the 24th IAEA Fusion Energy Conference 2012, San Diego, US.

General Remarks: An objective of this paper was to determine whether a good fit to a large variety of data is possible by Eq. 4. Nonetheless, it was regarded essential that the sets have approximately constant NBI heating and gas fuelling, and that they have approximately constant central density, and energy confinement. As discussed in the main text, datasets whose ELM waiting time pdf have two or more clear maxima of comparable sizes are not included. Some plasmas also have (approximately constant) ICRH heating during the time period analysed.

In the following tables of data, the first column is the JET pulse number, t_1 and t_2 give the time at which the time series analysis of D_α data started and ended respectively, B_T is the toroidal field in Tesla, I_p is the toroidal plasma current in Mega Amps, the other parameters are defined in the main text.

Type I (continued overpage)												
Shot	t ₁	t ₂	$\alpha=t_m/t_0$	β	c_W	μ	σ/μ	c_G	n	$\Lambda^{1/n}$	B_T	I_p
50564	62.0	67.0	0.00E+00	5.76	0.74	0.50E-01	0.19	0.69	100	0.98	1.9	1.9
52149	59.0	62.0	0.14E+01	4.07	0.70	0.45E-01	0.10	0.65	66	0.99	2.68	2.5
52508	59.5	63.0	0.21E-02	1.87	0.93	0.60E-01	0.55	0.95	57	1.05	2.6	2.4
52511	59.8	62.8	0.00E+00	6.97	0.29	0.31E-01	0.18	0.42	97	1.05	2.6	2.4
52513	59.5	62.8	0.63E+00	3.20	0.23	0.23E-01	0.20	0.24	142	1.01	2.6	2.4
52516	59.8	62.8	0.20E+00	3.40	0.36	0.24E-01	0.25	0.30	124	0.98	2.4	2.3
52517	59.8	62.8	0.10E+01	2.25	0.55	0.46E-01	0.22	0.59	64	1.03	2.4	2.3
52518	59.8	62.8	0.10E+01	2.51	0.95	0.68E-01	0.20	0.95	43	1.02	2.4	2.3
52519	60.7	63.7	0.00E+00	3.55	0.78	0.50E-01	0.32	0.76	59	0.95	2.4	2.3
52521	60.7	63.7	0.00E+00	4.25	0.71	0.50E-01	0.26	0.69	58	0.98	2.4	2.3
53142	59.0	63.8	0.11E+01	1.84	0.35	0.27E-01	0.25	0.53	176	1.09	2.4	2.3
56128	59.0	62.5	0.00E+00	6.44	0.70	0.39E-01	0.18	0.65	90	1.01	2.7	2.5
56143	59.0	62.0	0.15E+01	2.30	0.81	0.43E-01	0.17	0.80	68	1.03	2.7	2.5
56144	59.5	63.3	0.15E+01	2.12	0.61	0.35E-01	0.19	0.56	105	1.04	2.7	2.5
56739	62.5	67.0	0.65E+00	4.55	0.64	0.57E-01	0.14	0.59	78	0.99	1.4	1.4
56740	63.5	67.0	0.14E+01	1.92	0.62	0.19E-01	0.22	0.74	185	1.09	1.4	1.4
57861	59.0	63.3	0.00E+00	8.35	0.29	0.28E-01	0.15	0.49	150	1.06	2.7	2.5
57863	59.0	63.3	0.00E+00	3.45	0.84	0.41E-01	0.32	0.80	105	0.96	2.7	2.5
57865	59.0	63.3	0.00E+00	3.09	0.81	0.41E-01	0.35	0.77	104	0.96	2.7	2.5
57866	59.0	63.3	0.11E+01	1.83	0.43	0.35E-01	0.26	0.51	123	1.07	2.7	2.5
57870	59.0	63.3	0.26E+00	3.96	0.75	0.29E-01	0.23	0.78	146	1.02	2.7	2.5
57871	59.0	63.3	0.00E+00	5.04	0.82	0.30E-01	0.25	0.91	141	1.05	2.7	2.5
57872	59.0	63.3	0.32E+01	1.78	0.99	0.65E-01	0.13	1.01	65	1.09	2.7	2.5
57877	59.8	62.8	0.18E+01	2.65	0.49	0.56E-01	0.14	0.54	53	1.02	2.7	2.5
57885	59.0	62.8	0.40E-01	3.66	0.44	0.42E-01	0.28	0.41	89	0.98	2.7	2.5
57886	59.0	62.5	0.20E+01	2.20	0.60	0.48E-01	0.14	0.66	71	1.04	2.7	2.5
57888	59.0	62.8	0.29E-01	2.63	0.84	0.40E-01	0.35	0.68	95	0.97	2.7	2.5
57896	59.5	63.0	0.32E-01	3.58	0.64	0.33E-01	0.26	0.52	104	0.94	2.7	2.5
59354	60.0	63.5	0.73E+00	1.96	0.58	0.42E-01	0.29	0.62	83	1.08	2.7	2.5
60584	54.5	58.4	0.00E+00	3.48	0.67	0.54E-01	0.31	0.63	71	0.96	2.16	2.75
60709	60.0	63.8	0.00E+00	6.64	0.37 ₃	0.33E-01	0.18	0.41	113	1.02	2.7	2.5
61471	59.0	63.5	0.10E+01	3.18	0.65	0.23E-01	0.15	0.50	197	0.97	2.7	2.5

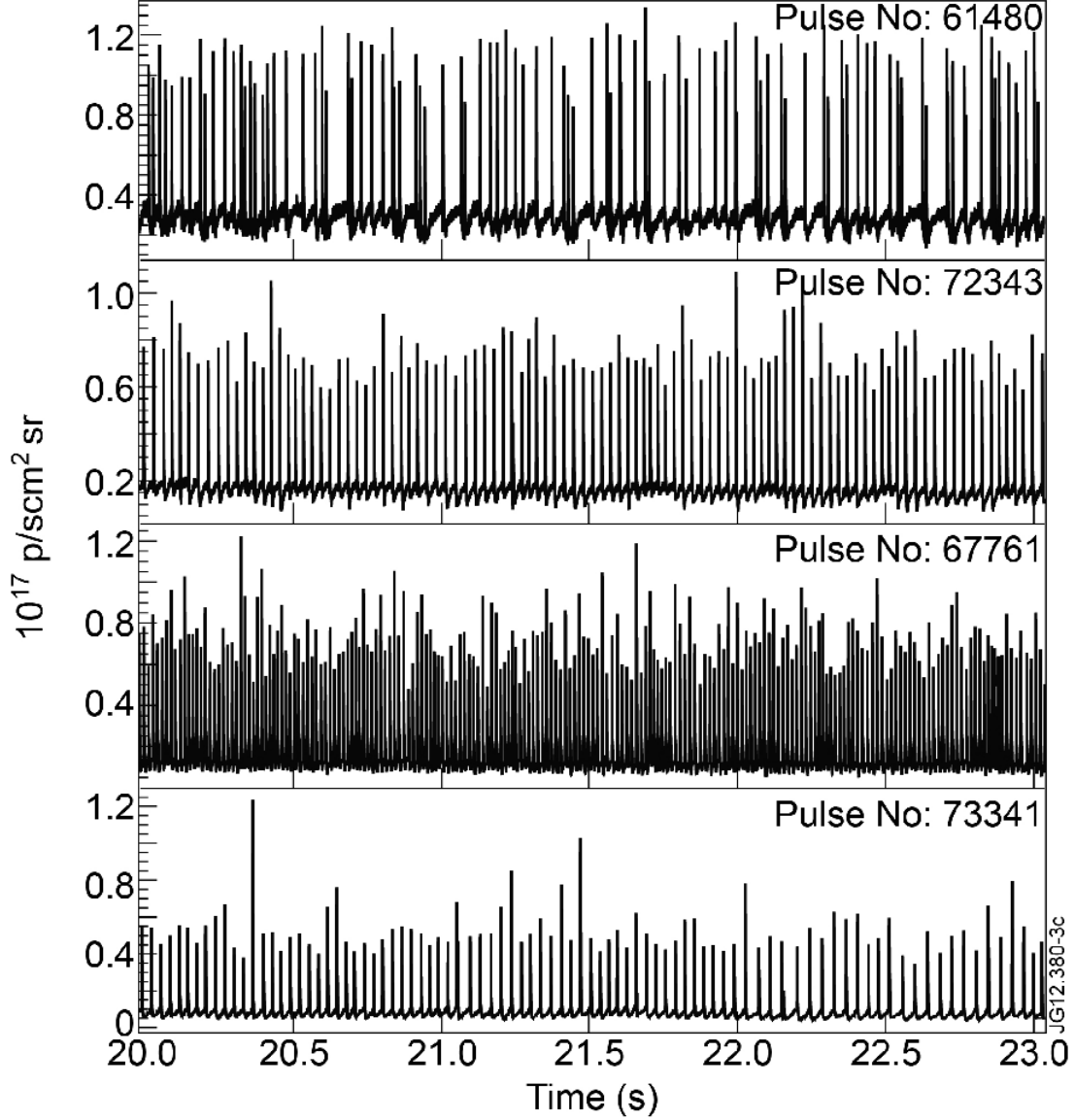


Figure 1: Example D_α time traces are shown for JET pulses (from the top down): 61480 ($\alpha = 0.02$, $\beta = 1.8$), 72343 ($\alpha = 0.0$, $\beta = 9.2$), 67761 ($\alpha = 1.2$, $\beta = 6.0$), and 73341 ($\alpha = 2.8$, $\beta = 1.9$).

For illustrative purposes, Figure 1 includes a selection of D_α time traces. The examples are chosen from the four extremities of our α - β plot in Figure 3 of the main text, and are shown for the time period of 60s-63s. The 60s-63s time window was chosen because it is included in the analysis of all the four pulses shown. From top to bottom in Figure 1, or clockwise from bottom left in the D_α plot of Figure 3 of the main text, the pulses are: 61480 ($\alpha = 0.02$, $\beta = 1.8$), 72343 ($\alpha = 0.0$, $\beta = 9.2$), 67761 ($\alpha = 1.2$, $\beta = 6.0$), and 73341 ($\alpha = 2.8$, $\beta = 1.9$).

Type I (continued)												
Shot	t ₁	t ₂	$\alpha=t_m/t_0$	β	c_W	μ	σ/μ	c_G	n	$\Lambda^{1/n}$	B_T	I_p
61472	59.0	63.5	0.16E+00	5.12	0.23	0.23E-01	0.18	0.16	195	0.98	2.7	2.5
61478	56.7	59.7	0.10E+00	2.20	0.45	0.25E-01	0.43	0.46	120	1.03	2.5	3.0
61479	59.5	63.5	0.00E+00	6.80	0.25	0.24E-01	0.18	0.38	166	1.04	2.75	2.5
61480	60.0	63.0	0.17E-02	1.75	0.79	0.31E-01	0.58	0.84	96	1.07	2.7	2.5
62216	60.0	63.0	0.24E-01	3.17	0.61	0.34E-01	0.34	0.62	86	1.01	2.4	2.0
62220	57.0	61.0	0.00E+00	3.46	0.86	0.61E-01	0.30	0.79	65	0.92	3.0	3.0
62221	57.0	61.0	0.00E+00	5.86	0.68	0.48E-01	0.19	0.63	84	0.98	3.0	3.0
62222	57.5	60.5	0.60E-01	1.90	0.77	0.34E-01	0.51	0.77	86	1.04	3.0	3.0
62224	57.5	61.0	0.00E+00	2.18	0.76	0.32E-01	0.48	0.75	110	1.02	3.0	3.0
66111	58.0	63.0	0.00E+00	5.99	0.62	0.32E-01	0.22	0.78	154	1.05	2.7	2.5
66115	58.0	63.0	0.00E+00	3.94	0.85	0.30E-01	0.31	0.88	168	0.97	2.7	2.5
66116	59.0	63.0	0.83E+00	6.84	0.10	0.22E-01	0.09	0.21	184	1.03	2.7	2.5
67761	59.5	63.0	0.12E+01	5.99	0.18	0.15E-01	0.09	0.16	234	1.01	2.7	2.5
69373	63.5	66.5	0.77E+00	2.44	0.54	0.38E-01	0.23	0.55	79	1.02	1.7	2.0
69900	55.5	59.3	0.62E-01	1.65	0.67	0.44E-01	0.57	0.68	86	1.09	2.8	3.0
70050	56.0	59.7	0.00E+00	2.47	0.56	0.32E-01	0.43	0.54	115	0.99	2.9	3.0
72339	59.0	63.0	0.11E+01	4.18	0.54	0.38E-01	0.12	0.49	103	0.99	2.7	2.5
72343	58.5	63.3	0.00E+00	9.20	0.43	0.31E-01	0.13	0.32	155	1.02	2.7	2.5
72345	60.0	63.0	0.17E+00	3.19	1.32	0.26E-01	0.23	1.02	113	0.90	2.7	2.5
73087	59.5	63.3	0.27E-01	5.59	0.92	0.32E-01	0.18	0.78	117	0.95	2.7	2.5
73335	59.0	63.0	0.44E+00	3.34	0.84	0.28E-01	0.20	0.72	144	0.96	2.7	2.5
73341	59.0	63.0	0.28E+01	1.87	0.65	0.35E-01	0.13	0.90	114	1.09	2.7	2.5
73345	59.5	63.0	0.70E+00	4.57	0.43	0.34E-01	0.14	0.44	103	1.01	2.7	2.5
73346	59.0	63.0	0.80E+00	4.45	0.43	0.31E-01	0.13	0.36	130	0.98	2.7	2.5
75722	65.0	69.5	0.51E+00	1.89	0.74	0.21E-01	0.36	0.84	216	1.13	1.6	1.5
75727	64.0	69.0	0.00E+00	4.52	0.91	0.58E-01	0.26	0.92	85	0.97	2.0	2.0
75731	64.5	67.5	0.41E+00	2.81	0.71	0.47E-01	0.27	0.73	62	1.02	2.0	2.0
75732	64.5	67.5	0.25E+00	2.93	0.59	0.43E-01	0.29	0.59	69	1.01	2.0	2.0
76473	58.5	61.5	0.18E+00	5.13	0.61	0.39E-01	0.18	0.55	76	0.99	2.0	2.0
76474	58.0	61.5	0.00E+00	6.14	0.72	0.40E-01	0.19	0.75	87	1.03	2.0	2.0
76475	58.5	61.5	0.00E+00	3.71	0.79 ₅	0.39E-01	0.32	0.80	76	0.99	2.0	2.0
76476	58.5	61.5	0.00E+00	2.81	0.97	0.39E-01	0.40	0.94	76	1.00	2.0	2.0

Type I (continued)												
Shot	t_1	t_2	$\alpha=t_m/t_0$	β	c_W	μ	σ/μ	c_G	n	$\Lambda^{1/n}$	B_T	I_p
76478	58.5	61.5	0.00E+00	3.81	0.51	0.38E-01	0.31	0.52	78	1.00	2.0	2.0
76479	58.0	62.0	0.00E+00	2.50	0.58	0.32E-01	0.42	0.55	124	1.00	2.0	2.0
76480	58.0	61.3	0.00E+00	2.70	0.44	0.29E-01	0.40	0.42	110	1.01	2.0	2.0
76481	58.0	61.5	0.00E+00	4.26	0.88	0.47E-01	0.26	0.85	73	0.99	2.0	2.0
76483	58.0	61.5	0.33E-02	2.22	0.55	0.29E-01	0.47	0.52	120	1.03	2.0	2.0

Type III ELMs												
Shot	t_1	t_2	$\alpha = t_m/t_0$	β	c_W	μ	σ/μ	c_G	n	$\Lambda^{1/n}$	B_T	I_p
68608	62.0	67.0	0.30E+00	1.17	0.26	0.82E-02	0.68	0.91	609	1.39	2.4	2.0
68610	60.5	66.0	0.17E+00	1.23	0.60	0.12E-01	0.77	1.23	475	1.44	2.4	2.0
68612	60.5	66.0	0.62E-01	1.30	0.98	0.14E-01	0.83	1.35	395	1.43	2.4	2.0
68613	60.5	66.0	0.17E+00	1.32	0.70	0.14E-01	0.71	1.10	385	1.36	2.4	2.0
68614	60.5	66.0	0.17E+00	1.17	0.98	0.14E-01	0.90	1.62	395	1.65	2.4	2.0
68615	60.5	66.0	0.19E+00	1.30	0.83	0.13E-01	0.71	1.27	421	1.39	2.4	2.0
68618	60.5	66.0	0.13E+00	1.37	0.61	0.12E-01	0.70	1.08	445	1.32	2.4	2.0
68619	60.5	66.0	0.24E+00	1.22	0.78	0.13E-01	0.75	1.45	438	1.48	2.4	2.0
74410	56.0	60.5	0.34E+00	1.04	0.57	0.18E-01	0.74	1.33	250	1.53	2.0	2.5
74411	56.0	60.5	0.12E+00	1.11	0.51	0.15E-01	0.90	1.27	297	1.55	2.0	2.5
74412	56.0	60.5	0.77E-01	1.00	0.88	0.17E-01	0.97	1.14	263	1.58	2.0	2.5
74415	56.0	60.5	0.68E-01	1.00	0.85	0.14E-01	1.00	1.29	315	1.61	2.0	2.5
74417	57.0	60.5	0.90E-01	1.00	0.52	0.10E-01	1.08	1.34	334	1.77	2.0	2.5
74427	56.0	60.5	0.93E-01	1.00	1.06	0.18E-01	1.12	1.65	249	1.83	2.0	2.5
74428	57.0	60.5	0.10E+00	1.22	0.32	0.11E-01	0.75	0.71	313	1.30	2.0	2.5

“High frequency” type I ELMs												
Shot	t_1	t_2	$\alpha = t_m/t_0$	β	c_W	μ	σ/μ	c_G	n	$\Lambda^{1/n}$	B_T	I_p
66109	59.0	63.0	0.00E+00	3.39	0.62	0.92E-02	0.30	0.51	435	0.96	2.7	2.5
66108	59.0	62.5	0.00E+00	2.50	0.90	0.89E-02	0.40	0.80	390	0.99	2.7	2.5
66107	59.0	63.0	0.56E-01	3.73	0.48	0.83E-02	0.23	0.32	480	0.92	2.7	2.5
66106	59.0	63.0	0.41E+00	2.70	0.37	0.12E-01	0.26	0.43	328	1.01	2.7	2.5
66105	59.0	63.0	0.11E+00	3.63	0.48	0.83E-02	0.23	0.26	479	0.92	2.7	2.5